HHS Public Access

Author manuscript

Gene Ther. Author manuscript; available in PMC 2011 December 01.

Published in final edited form as:

Gene Ther. 2011 June ; 18(6): 569–578. doi:10.1038/gt.2010.175.

Adeno-associated virus-mediated gene delivery into the scala media of the normal and deafened adult mouse ear

Lauren A. Kilpatrick[1], **Qian Li**[2], **John Yang**[1], **John C Goddard**[3], **Donna M. Fekete**[4], and **Hainan Lang**[2,*]

[1] Department of Otolaryngology – Head & Neck Surgery, Medical University of South Carolina, Charleston, SC 29425, United States

[2] Department of Pathology and Laboratory Medicine, Medical University of South Carolina, Charleston, SC 29425, United States

[3] House Ear Clinic, Los Angeles, CA 90057, United States

[4] Department of Biology Science, Purdue University, Lafayette, IN 47907, United States

Abstract

Murine models are ideal for studying cochlear gene transfer as many hearing loss-related mutations have been discovered and mapped within the mouse genome. However, due to its small size and delicate nature, the membranous labyrinth of the mouse is a challenging target for delivery of viral vectors. To minimize injection trauma, we developed a procedure for the controlled release of adeno-associated viruses (AAV) into the scala media of adult mice. This procedure poses minimal risk of injury to structures of the cochlea and middle ear and allows for near-complete preservation of low and middle frequency hearing. In the present study, transduction efficiency and cellular specificity of AAV vectors (serotypes 1, 2, 5, 6, and 8) were investigated in normal and drug-deafened ears. Using the cytomegalovirus (CMV) promoter to drive gene expression, a variety of cell types were transduced successfully, including sensory hair cells and supporting cells, as well as cells in the auditory nerve and spiral ligament. Among all five serotypes, inner hair cells (IHCs) were the most effectively transduced cochlear cell type. All five serotypes of AAV vectors transduced cells of the auditory nerve, though serotype 8 was the most efficient vector for transduction. Our findings indicate that efficient AAV inoculation (via the scala media) can be performed in adult mouse ears, with hearing preservation a realistic goal. The procedure we describe may also have applications for intra-endolymphatic drug delivery in many mouse models of human deafness.

Keywords

AAV vectors; scala media; gene therapy; sensory hair cells; auditory nerves; hearing loss

Corresponding author: Hainan Lang, Department of Pathology and Laboratory Medicine, Medical University of South Carolina, 165 Ashley Avenue, PO BOX 250908, Charleston, SC 29425, USA, Tel: 843-792-2711, Fax: 843-792-0368, langh@musc.edu.

Conflict of interest

The authors declare no conflict of interest.

Introduction

Hearing loss is largely due to degeneration and/or abnormality of sensory hair cells, spiral ganglion neurons, or specific non-sensory cells, such as fibrocytes in the spiral ligament and glial cells in the auditory nerve. In mammalian vertebrates, sensory hair cells and spiral ganglion neurons are unable to regenerate from surviving cell populations. There is evidence that certain non-sensory cells, such as cochlear fibrocytes, are able to repopulate themselves after injury; however, this regenerative ability declines with age.[1,2,3] Non-mammalian vertebrates can replace lost hair cells through direct and indirect trans-differentiation of supporting cells (see review from Brignull et al[4] and Groves[5]). Raphael's group developed an adult guinea pig model of cochlear cell regeneration using adenoviral vectors to drive expression of the Atoh1 transcription factor in the drug-damaged organ of Corti, leading to a remarkable recovery of auditory function and regeneration or repair of drug-damaged hair cells.[6] Staecker et al[7] found that Atoh1 gene transfer using adenovectors resulted in the recovery of vestibular function and regeneration of macular hair cells. Gubbels et al[8] reported that Atoh1 gene transfer is able to induce functional hair cells in the mouse cochlea using *in utero* electroporation of plasmid DNA. These and other gene transfer studies in the inner ear demonstrate the feasibility of genetic manipulation for cell replacement based on inducing regeneration and/or trans-differentiation of endogenous cochlear cells. In the past 15 years, numerous studies have investigated the functional and structural effects of gene transfer into inner ear tissues.[9–43] These reports have provided important information on the advantages and disadvantages of different surgical approaches, gene delivery methods and viral vectors.

AAV has limited immunogenicity and toxicity and has been shown in previous studies to transduce cochlear hair cells and supporting cells (SCs).[9,14,24,25,27,32,37,42,43] To date, the majority of these studies have used primary mouse cochlear explants, perinatal mouse cochleas, or adult guinea pig cochleas as models to investigate the transduction efficiency of AAV vectors. Adult mice present an ideal model for cochlear gene transfer because their genetic information is accessible and many hearing loss-related mutations have been discovered. Via a scala tympani approach in normal adult mice, Liu et al[25] successfully transduced inner hair cells (IHCs) and other cochlear cell types including cells in the spiral ligament and the spiral ganglion using AAV vectors. However, no outer hair cells (OHCs) and only a few SCs were seen for all 8 AAV serotypes examined.

Further improvement in infection efficiency of OHCs and SCs in the mouse model is desirable, especially since the therapeutic delivery of genes to specific inner ear cells may be required to treat different genetic causes of deafness. In the present study, we examined the efficiency of AAV infectivity of IHCs, OHCs, SCs, auditory nerve fibers, and cells of the lateral wall under various conditions. More specifically, transduction efficiency was assessed in the presence or absence of drug-induced hair cell loss as well as under various conditions (serotypes, volume, rate) of virus delivery into the scala media. The delivery of fluid reagents into the scala media is particularly challenging in the mouse due to its small volume and the need to add an appropriate number of transducing viral particles to ensure efficient infection. To reduce the surgical trauma to cochlear cells associated with bulk fluid

injections, we employed a newly-developed nanoliter-level fluid delivery system (Nanoliter Microinjection System, WPI, Sarasota, FL). Using this system, injection trauma can be minimized by optimizing the delivered volume while reducing the speed of injection. A variety of cell types in normal and deafened inner ears were successfully transduced including sensory cells in the organ of Corti, cells in the auditory nerve and the spiral ligament of the cochlear lateral wall, as well as cells in the vestibular end organs.

Results

Rapid hearing loss and outer hair cell loss in kanamycin- and furosemide-treated adult mice

To optimize the use of AAV vectors for therapeutic treatment of hair cell loss, it was important to compare virus-mediated gene transduction in normal and damaged ears of adult mice. For deafening, we employed a recently published method of rapid hair cell degeneration that used a combination of a single dose of aminoglycoside following by a single dose of a loop diuretic delivered intraperitoneally into adult CBA/CaJ mice.[45,49,50] Auditory brainstem responses (ABRs) were measured at 3 days, 7 days, 1 month, or 3–5 months after treatment (Fig. 1a). A significant ABR threshold shift (about 40–70 dB SPL across all tested frequencies) was revealed as early as 3 days after treatment. No signs of functional recovery were seen at 3–5 months after treatment, which was the longest recovery period examined.

Drug-treated mice were examined at 7 days, 1 month and 3 months to evaluate the extent of hair cell destruction. A loss of OHCs was seen in the entire basal turn and most of the apical turn of the examined ears (n=19) (Figs. 1b, 1c, 1d). Only a small number of OHCs remained in the extreme apex. The majority of IHCs were intact but a scattered loss of IHCs was observed in the basal turns of treated mice. These results correspond with previous studies.[45,49,50] Most importantly, relatively normal architecture of supporting cells was seen 1–3 months after treatment (Figs. 1d, 1e). Therefore, this deafened model is ideal for testing the transduction efficiency of AAV viruses in surviving supporting cells in the context of nearly complete OHC loss.

Scala media inoculation with limited surgical trauma

The organ of Corti is a delicate epithelium located on the basilar membrane, an acellular structure suspended across a fluid-filled space deep within the temporal bone. Furthermore, delivery of virus directly to the apical surfaces of the sensory epithelium requires a breach of the scala media, a tubular compartment filled with potassium-rich endolymphatic fluid. Excessive leakage of endolymph at the site of injection will degrade the transepithelial endocochlear potential that is an essential driving force for effective mechanosensory transduction. To better preserve the integrity of both the basilar membrane and the organ of Corti, we established a surgical approach to deliver AAV vectors into the scala media through the lateral wall (Fig. 2a, 2b). The bulla was surgically exposed and prepared to permit access to the basal turn of the mouse ear. This approach allows direct visualization of the bony lateral wall of the scala media and the richly vascularized spiral ligament of the stria vascularis that lies just beneath. We were able to minimize injection trauma by

optimizing the delivered volume and speed of injection through glass micropipettes using a Nanoliter Microinjection System. Although injection trauma was minimal, 7% of animal subjects showed significant leakage of endolymph at the injection site and thus were not included in the study.

Physiological assessments were used to evaluate whether the surgical procedure itself was potentially damaging to the inner ear. Figures 2c and 2d show that no significant ABR threshold shifts were seen at 4 to 22.6 kHz in a normal mouse 7 days after AAV inoculation. However, a 30–40 dB SPL shift in the ABR threshold did appear at higher frequencies (32, 40 and 45.2 kHz), suggesting a cochlear injury at the extreme basal turn adjacent to the typical injection site. In contrast, deafened mice, which were already missing most OHCs and some IHCs in the basal turn (data not shown), demonstrated no additional high-frequency ABR threshold shifts in response to virus inoculation (Fig. 2e)

Transduction efficiency of five AAV serotypes in the normal and deafened mouse ears

Five types of AAV-GFP vectors (serotypes 1, 2, 5, 6, and 8) were delivered to normal or deafened adult mice. Although histological analysis revealed that many cell types could express GFP following AAV inoculation, IHCs were by far the most commonly transfected (Figs. 3 and 4). For a semi-quantitative evaluation of the relative transduction efficiency of AAVs under different experimental conditions, we counted IHC expression in two different ways. First, the number of mice showing any GFP expression in IHCs was counted relative to the total number of mice inoculated. Second, the number of mice with more than 100 GFP^+ IHCs was counted and compared to the total number of mice inoculated. Both of these measures can be found in Table 1 for the full set of inoculated animals.

The epithelium of a deafened animal is likely to differ from that of a normal animal, and these changes might influence the number or types of cells infected under the two conditions. Furthermore, an acutely deafened organ of Corti may not necessarily be infected with similar efficiency to that which is chronically deafened. To examine the effects of post-deafening recovery time, AAV was delivered into the scala media of the deafened cochlea following either short term (3–7 days, acutely-deafened) or long term (1–6 month, chronically-deafened) recovery periods after kanamycin and furosemide treatment. There is a trend showing that AAV transduction is more effective in acutely-deafened mice than chronically-deafened mice (Table 1). About 87% (32/37) of the acutely-deafened mice expressed GFP protein, as compared to 68% (17/25) of the chronically-deafened mice. This compares to 88% (35/39) of normal animals that were transduced with GFP. However, these numbers do not take into account the rather large differences in infection efficiency across viral serotypes.

For each AAV serotype, we initially examined 3–4 animals per group. The overall transduction efficiency showed that GFP transduction was best achieved with serotypes 2 and 8, secondarily with serotype 6 and lastly with serotypes 1 and 5. The initial results led us to focus on serotypes 2 and 8 to further examine the effect of survival time after virus inoculation on the transduction efficiency (Tables 1 and 2). The transduction patterns of AAV vectors in sensory cells of normal and deafened ears were also characterized using vector serotypes 2 and 8 (Figs. 5 and 6).

The effect of recovery period on transduction efficiency of AAV was compared for serotypes 2 and 8 at seven days and one month after surgery (Table 2). The percentage of inoculated mice showing any GFP expression in IHCs ranges from 88–100%, with no clear advantage of one serotype over the other using this measure. The percentage of inoculated mice with >100 GFP^+ IHCs shows a large range from 41–64%, with the highest percentage seen at one month for serotype 2. Qualitatively, there was no clear trend towards a larger number of GFP-expressing cells per ear with increased recovery time.

AAV transduction in the auditory organ of normal and deafened mice

For all five AAV serotypes, IHCs were the most effectively transduced cell type in the organ of Corti. Robust expression of GFPin IHCs was seen in both normal and deafened mice, especially for serotypes 2 and 8 (Figs. 3 and 4). Figure 4a shows a deafened mouse with near complete IHC transduction 7 days after serotype 2 virus inoculation. OHCs were also shown to express GFP in the normal ear (Fig. 3). However, robust GFP^+ OHCs were only seen in the apical turns of four normal mice (out of 25 mice that were inoculated with serotype 2 and 8 viruses).

A small number of GFP^+ SCs were seen in normal and deafened mice for serotypes 2, 6 and 8 (Figs. 3d, 3e, 4e, 5a–f). Sox2 was used as a marker to identify SCs. A previous study has indicated that Sox2 can be expressed in the nuclei of all cochlear SC subtypes including Deiters', Hensen's, inner and outer pillars, inner phalangeal, and border cells.[45] Figure 5 reveals that some of the GFP^+ cells were co-labeled with Sox2. However, there are some GFP^+ cells in the SC region (outer pillar cell region) of the deafened mice that were not stained for Sox2 (Figure 5). It is possible that these $GFP^+/Sox2^-$ cells are fibroblasts or macrophages that appeared in response to the loss of cochlear OHCs.

AAV transduction in the vestibular organs of normal and deafened mice

We were also interested in whether scala media inoculation could yield GFP gene transduction in vestibular organs. The examination of frozen sections of the inner ears of normal and deafened mice revealed GFP expression in both a subset of HCs and SCs of the sensory epithelia of vestibular organs including the macula and ampulla (Figure 6). Oesterle et al[45] reported that Sox2 protein was expressed in SCs and type II HCs of both the striolar and extra-striolar regions. We found that a majority of the GFP^+ HCs were co-labeled with Sox2, suggesting these cells are type II HCs (Fig. 6c–h). GFP expression patterns were similar in normal and deafened ears. A few GFP^+ cells were also seen within the stromal region of the vestibular organs (data not shown).

AAV transduction in the auditory nerve and cochlear lateral wall of normal and deafened mice

Scala media inoculation can also produce efficient GFP transduction in cells within Rosenthal's canal, although this region was not specifically targeted. Based upon their morphological features, GFP^+ cells within Rosenthal's canal are mostly glial cells (Fig. 7). The proportion of normal and deafened animals showing GFP expression as a function of viral serotype is shown in Table 3. Transduction was best achieved with serotype 8. GFP^+ auditory nerve cells were seen in 60% of inoculated mice for serotype 8, 43% for serotype 1,

42% for serotype 3, 38% for serotype 6 and 22% for serotype 5. Overall, we observed a trend towards higher transduction efficiency in deafened ears as compared to normal ears.

GFP^+ cells were also seen in the spiral ligament of normal and deafened mice that received serotypes 2 and 8 viruses (Fig. 8). In most cases, GFP was expressed in the outer sulcus epithelial cells as well as type II and IV fibrocytes of the spiral ligament. GFP^+ fibrocytes were mostly located in the basal turns of both normal and deafened mice. No GFP^+ cells were seen in the stria vascularis of the specimens examined.

Discussion

An optimized scala media delivery approach for adult mouse inner ear

We established a scala media delivery procedure that is able to target a variety of cell types in normal and deafened adult mouse ears. The cell types transduced include sensory HCs and SCs in the auditory and vestibular organs as well as glial cells in the auditory nerve and fibrocytes of the spiral ligament. Most importantly, this procedure minimizes surgical trauma and preserves hearing, especially at low and middle frequencies. Compared to previous studies that have used a scala media approach, there were two major improvements in our procedure which played an important role in reducing cochlear injury and preserving hearing. First, a nanoliter-level fluid delivery system was used to control the precisely delivered volume and speed of virus injection. This system allows us to deliver controlled amounts of fluid as small as 4.6 nl. In the adult mouse, the volume of the endolymphatic space in the scala media was reported to be 0.19 μl.[51] In our procedure, multiple injections were performed and the fluid volume delivered into the scala media was approximately 46 nl per injection. There was a one-minute recovery period after each injection, allowing the host cochlear cells to adjust to the change in endolymphatic pressure. A slow-infusion technique with a minor disruption to the cochlear fluid environment during virus inoculation is critical for delivering virus into the endolymph compartment with minimal tissue trauma. A similar strategy was used for fluid delivery into the perilymph compartment of the adult mouse cochlea.[52], [53] Infusion of an artificial perilymph solution into the scala tympani at a rate of 16–32 nl/min resulted in good preservation of hearing function.

Second, our surgical method was adopted from a standard non-invasive procedure of endocochlear potential measurement in adult mice.[54] The bony lateral wall of the scala media was thinned by a dental drill but the membranous lateral wall was left intact. The endolymph-filled cavity was sealed completely without an opening hole during the surgical procedure. This preparation allows the sharp tip of a glass micropipette to penetrate the membranous lateral wall of the scala media without endolymph leakage. By the end of the virus delivery procedure, the penetrated site was able to completely close after the micropipette was removed.

A great advantage of the scala media approach is the highly efficient transduction of cochlear sensory cells.[6], [21],[24] The improved delivery methods developed in this study largely reduced cochlear injury and preserved low and middle frequency hearing well following scala media virus inoculation. This delivery procedure may potentially be used for intra-endolymphatic drug delivery in various mouse models of human deafness.

IHCs were most effectively transduced by AAV vectors

AAV vectors have often been used for gene delivery into the central nervous system as they express genes in post-mitotic neuronal cells for long periods with minimal to no immunogenicity and toxicity (see review from Hester et al.[55]). An interesting finding in this study is that IHCs, the post-mitotic sensory cells of the inner ear, were most effectively transduced by AAV vectors. This finding is of value for further molecular and physiological studies of sensory hair cells and for planning gene therapy strategies when deafness is caused by a gene deficit in sensory hair cells that does not affect their survival but perturbs their function.

GFP^+ IHCs were seen in ears inoculated with all five serotypes of AAV vectors (serotypes 1, 2, 5, 6 and 8). In particular, AAV2 and AAV8 were the most efficient vectors for IHC transduction. The divergence of cellular tropism observed in AAV serotype vectors may contribute to the differential characteristics of the vector-cell interaction. It has been known that transduction of cells with AAV2 is mediated by heparan sulphate proteoglycan receptor, fibroblast growth factor receptor 1, aVb5.[56–58] Like AAV2, AAV8 also needs a laminin receptor for cell entry.[58] In contrast to those two serotypes, AAV1, AAV5 and AAV6 do not need to bind a receptor for cell entry.[58,59] Interestingly, our study found that a majority of the GFP^+ HCs in vestibular organs are type II HCs ($Sox2^+$) suggesting that type II vestibular HCs may share a common AAV8 receptor (such as a laminin receptor) with cochlear IHCs.

The use of the CMV promoter may also contribute to the high transduction pattern seen in cochlear IHCs. A previous study showed that replication-defective (E1−, E3−, pol−) adenovirus vectors containing CMV-driven LacZ can transduce about 99% of the IHCs in the basal turn and 90% of the IHCs in the apical turn of adult guinea pigs.[23] Liu et al.[25] reported that AAV serotype 3 vectors containing chicken β-actin promoter can transduce adult mouse IHCs with high efficiency. It will be interesting to examine whether AAV3 with the CMV promoter can produce a similar gene transduction pattern.

Cochlear supporting cells can be transduced although their transduction rate is relatively low

We expected the infection efficiency of SCs to be enhanced by drug treatment, since the absence of HCs should allow the apical surfaces of SCs to expand and thus present a larger apical surface area for binding of viral particles. While GFP^+ SCs were seen in both normal and deafened mouse ears inoculated with AAV2, AAV6 and AAV8, the transduction efficiency of SCs was low in both conditions. Furthermore, there was no difference in SC infectivity comparing short-term (acutely deafened ears) and long-term (chronically deafened ears) recovery periods after kanamycin and furosemide treatment. Thus, OHC loss does not appear to increase gene transduction efficiency into SCs. These results suggest that either receptor availability is limiting, or perhaps the CMV promoter is not an ideal promoter for expression in adult SCs. Previous studies reported robust transgene expression in cochlear SCs of several models including mouse cochlear explants, postnatal mouse ear and adult guinea pig ear. Stone et al[26] found that the GFAP promoter with AAV serotypes 1 and 2 vectors can result in strong transgene expression in SCs of the cultured organ of Corti taken from E13 or P0-1 mice. Iizuka et al[32] observed an efficient transgenesis in Deiter's

cells, IHCs, and lateral wall cells after AAV serotype 5 vectors with a CMV promoter were delivered into P0 mouse ears. Shibata et al[37] observed that bovine AAV with a β-actin promoter transduced SCs efficiently in both normal and deafened adult guinea pig cochleas. Our data and these previously reported data demonstrate that the SC transduction efficiency is likely dependent upon the choice of promoters, virus serotypes, *in vitro* or *in vivo* inoculation, animal species, and animal age. Further investigation into the proper promoter may be necessary to increase the efficiency of targeting SCs in the adult mouse ear with AAV vectors.

The transgene expression in the cells of the spiral ligament and auditory nerve

Another finding of this study is that scala media delivery of vectors can transduce GFP gene expression in fibrocytes of the spiral ligament of the cochlear lateral wall. Non-sensory cells such as fibrocytes, along with sensory hair cells and neurons, form the highly complex microarchitecture of the inner ear. Non-sensory cells not only provide an essential environment for the health of sensory hair cells and neurons, but they also play an important role in the maintenance of normal auditory functions.[60,61,62] The ability to transfer genes into the cells of the cochlear lateral wall is important for better understanding the function of cochlear fibrocytes.

This study also found that the scala media approach can transduce the GFP gene in glial cells of the auditory nerve. We compared the transduction efficiency of 5 serotypes of AAV vectors in the auditory nerve. Serotype 8 was found to be optimal for gene transfer in the auditory nerve under these experimental conditions. In addition, there is a trend toward an increased transduction efficiency into the nerve in deafened mice compared to normal mice. Local transduction of cochlear glial cells with a secreted protein, e.g., a growth factor, could prove beneficial for preventing the degeneration of spiral ganglion neurons after HC loss or with age. A recent study showed that transgene expression of the neurotrophin BDNF in cochleas with prior hair cell degeneration led to a robust re-growth of auditory nerve fibers into the sensory epithelium.[63]

Materials and methods

AAV vector construction and preparations

Purified AAV-GFP vectors of serotypes 1, 2, 5, 6, 8 were purchased from the Harvard Gene Therapy Initiative (Harvard Medical School, Boston, MA). Viral stocks were generated by tripartite transfection (AAV-RE/CAP expression plasmid, adeno-miniplasmid pHGTI-Adeno1 and AAV transfer vector plasmid pAAV-GF) into HEK293 cells. GFP expression in these vectors is driven by the CMV promoter. Serotype 2 particles were purified by heparin column chromatography. All other serotypes were purified by iodixanol density gradient followed by Q sepharose column chromatography. Purified vector particles were dialyzed extensively against PBS, concentrated by Amicon spin columns, and titered by dot blot hybridization. Concentrated virus titers for serotypes 1, 2, 5, 6 and 8 were 6.7×10^{12}, 3.2×10^{12}, 5.3×10^{12}, 7.5×10^{12} and 1×10^{13} genome copies per ml, respectively. With total injection volumes of ~322 nl per cochlea (see below), approximately $1–3 \times 10^{9}$ genomes were delivered to each ear. Previous work has shown that genome copies per ml, calculated

using quantitative polymerase chain reaction, can overestimate by ~5 log units the number of AAV transducing units/ml, based on LacZ or eGFP transgene expression following limiting dilutions on cultured cells.[44] Thus, we estimate that we are delivering approximately 10,000–30,000 transducing units to each ear.

Animals

A colony of adult CBA/CaJ mice was established with original breeding pairs purchased from the Jackson Laboratory (Bar Harbor, ME) and bred in-house in a low-noise environment at the Animal Research Facility of the Medical University of South Carolina (MUSC). About 120 mice of both genders, aged 2 to 12 months and weighing 16–35g, were used in the study. All aspects of the animal research were conducted in accordance with the guidelines of the Institutional Animal Care and Use Committee of MUSC. Prior to data acquisition, mice were examined for signs of external ear canal and middle ear obstruction. Mice with any symptoms of ear infection were excluded from the study.

Kanamycin and furosemide treatment

Cochlear lesions were induced according to a previous description by Oesterle et al.[45] Kanamycin sulfate (Sigma-Aldritch, St. Louis, MO) was dissolved in physiological saline to a concentration of 45 mg/ml. Mice were deafened with a single dose of kanamycin (1,000 mg/kg, subcutaneous) followed 45 min later by a single intraperitoneal injection of furosemide (400 mg/kg) (American Regent Laboratories, INC).

Physiological procedures

Mice were anesthetized by an intraperitoneal injection of xylazine (20mg/kg) and ketamine (100mg/kg) and placed in a head holder in a sound-isolation room. Young adult CBA/CaJ mice underwent physiological measurements before and after the kanamycin and furosemide treatment as well as before and after virus delivery. Auditory brainstem responses were recorded via customized needle electrodes inserted at the vertex (+) and test-side mastoid (−), with a ground in the control-side leg. The acoustic stimuli were generated using Tucker Davis Technologies equipment III (Tucker-Davis Technologies, Gainsville, FL, USA) and a SigGen software package. ABRs were evoked at half octave frequencies from 4 to 45 kHz with 5 ms duration tone pips with $\cos^2$ rise/fall times of 0.5 ms delivered at 31/s. At each sound level, 300–500 responses were averaged, using an “artifact reject” whereby response waves were discarded when peak-to-peak amplitude exceeded 50 mV. Physiological results were analyzed for individual frequencies, and then averaged for each of these frequencies from 4.0 to 40 kHz.

Surgical procedures for the scala media inoculation

Normal and deafened mice were anesthetized as described above. The bulla was exposed through a post-auricular approach and a small perforation was created to expose the basal portion of the cochlea. The bony cochlear lateral wall of the scala media in the basal turn was thinned carefully using a dental drill with a micro-burr. Note that a small area (about 30–40 μm in diameter) of the bony lateral wall at the basal turn was mostly removed by the dental drill, but the membranous lateral wall was intact. Glass micropipettes (WPI, Sarasota,

FL) were pulled and the tips were broken to a diameter of 15–20 μm. The Nanoliter Microinjection System (WPI, Sarasota, FL) was used to deliver controlled amounts of fluid. The injection speed was set for a rate of 46 nl/sec according to the manufacturer's protocol (http://www.wpiinc.com/index.php/vmchk/B203XVY.html). For each mouse, a total of seven injections were completed with a one-minute recovery period after each injection. The duration of one injection was about 1 sec, delivering a total of ~322 nl into the inner ear.

Morphological and immunohistochemical analysis

For morphological observation of the deafened ears, the anesthetized animals (7 days, 1 or 3 months after kanamycin and furosemide treatment) were perfused via cardiac catheter first with 10 ml of normal saline containing 0.1 % sodium nitrite and then with 15 ml of a mixture of 4% paraformaldehyde and 2% glutaraldehyde in 0.1M phosphate buffer, pH 7.4. After removing the stapes and opening the oval and round windows, 0.5 ml of fixative was perfused gently into the scala vestibuli through the oval window. The inner ears were dissected free and immersed in fixative overnight at 4 °C. Decalcification was completed by immersion in about 50 ml of 120 mM solution of ethylenediamine tetracetic acid (EDTA) for 2–3 days. The tissues were post-fixed with 1% osmium tetroxide for 1 hour, dehydrated and embedded in Epon LX 112 resin. Semi- thin sections approximately 1 μm thick were cut and stained with toluidine blue.

For direct observation of GFP-gene transduction and immunohistochemical analysis, the anesthetized animals were perfused via a cardiac catheter first with 10 ml of normal saline containing 0.1 % sodium nitrite in normal saline and then with 15 ml of 4% paraformaldehyde in 0.1M phosphate buffer, pH 7.4. The procedures for observation of surface preparations of the mouse cochleas have been described previously.[47] The cochlear sensory epithelium, modiolus, stria vascularis and spiral ligament were carefully dissected from the fixed cochlea. GFP^+ cells were directly observed and counted using either a Zeiss Axio Observer fluorescent microscope or a Zeiss LSM5 Pascal confocal microscope (Carl Zeiss Inc., Jena, Germany). All virus-injected right ears (n=101) were processed for morphological and/or immunohistochemical observation and are listed in Table 1. To investigate the possibility of contralateral transduction, 38 uninjected (left) ears were randomly selected from mice in the serotypes 2 and 8 groups and were also processed for direct observation of GFP-gene transduction. However, no GFP^+ cells were found in these cochleas. These uninjected ears were excluded from Tables 1, 2 and 3.

In some cases, the cochlear sensory epithelia were processed for dual-immunostaining for GFP and Sox2. These specimens were prepared according to the method previously described.[47] Frozen sections or surface preparations of cochlear tissue were blocked with 0.25% BSA and incubated overnight at 4°C with primary antibodies. The primary antisera were rabbit anti-GFP (1:200, A11120, Molecular Probes, Eugene, OR) and goat anti-Sox2 (1:200, sc17320, Santa Cruz Biotechnology, Santa Cruz, CA). Biotinylated secondary antibodies were detected with avidin D coupled to FITC (1:150) or Texas-red (1:150) (Vector, Burlingame, CA). Nuclei were counterstained with bisbenzimide or propidium iodide (PI) in specimens stained with only one primary antibody. Negative controls included omission of the primary antibody or substitution with similar dilutions of non-immune

serum of the appropriate species. No regionally specific staining was detected in any of these control experiments.

Anti-GFP rabbit polyclonal and mouse monoclonal antibodies raised against GFP isolated directly from the jellyfish *Aequorea victoria* have been used for detection of native GFP, GFP variants and most GFP fusion proteins[48]. The goat polyclonal antibody for Sox2 was raised against a peptide corresponding to C-terminus aa 227–293 of human origin (manufacturer's technical information). Western blot analysis revealed a single band at 34 kDa in human and mouse embryonic stem cell lysates.

The sections were examined either with a Zeiss Axio Observer or a Zeiss LSM5 Pascal confocal microscope (Carl Zeiss Inc., Jena, Germany). The captured images were processed using Image Pro Plus software (Media Cybernetics, MD), AxioVison 4.8 (Carl Zeiss Inc., Jena, Germany) and Zeiss LSM Image Browser Version 2,0,70 (Carl Zeiss Inc., Jena, Germany). Adobe Photoshop CS2 was employed to adjust brightness, contrast, and sharpness of images with identical setting for all panels. Alterations were not performed on images used for quantitative purposes.

Acknowledgments

Grant sponsors: National Institutes of Health; Grant number: DC00422 (H.L.); Grant number: DC07506 (H.L.); Grant number: DC00713 (B.A.S.); Grant number: DC002756 (D.M.F); American Academy of Otolaryngology-Head and Neck Surgery; Grant number: CORE 130165 (L.A.K.).

The authors thank Vinu Jyothi for her assistance in ototoxic drug exposure and ABR measurements; Manna Li, Juhong Zhu, Nancy Smythe and James Nicholson for their help with histological observations; Bradley A. Schulte and Richard A. Schmiedt for their critical comments and invaluable discussion over the course of this study.

References

1. Roberson DW, Rubel EW. Cell division in the gerbil cochlea after acoustic trauma. Am J Otol. 1994; 15(1):28–34. [PubMed: 8109626]
2. Yamashita H, Shimogori H, Sugahara K, Takahashi M. Cell proliferation in spiral ligament of mouse cochlea damaged by dihydrostreptomycin sulfate. Acta Otolaryngol. 1999; 119(3):322–5. [PubMed: 10380736]
3. Lang H, Schulte BA, Schmiedt RA. Effects of chronic furosemide treatment and age on cell division in the adult gerbil inner ear. J Assoc Res Otolaryngol. 2003; 4(2):164–75. [PubMed: 12943371]
4. Brignull HR, Raible DW, Stone JS. Feathers and fins: non-mammalian models for hair cell regeneration. Brain Res. 2009; 24(1277):12–23. [PubMed: 19245801]
5. Groves AK. The challenge of hair cell regeneration. Exp Biol Med (Maywood). 2010; 235(4):434–46. [PubMed: 20407075]
6. Izumikawa M, Minoda R, Kawamoto K, Abrashkin KA, Swiderski DL, Dolan DF, et al. Auditory hair cell replacement and hearing improvement by Atoh1 gene therapy in deaf mammals. Nat Med. 2005; 11(3):271–6. [PubMed: 15711559]
7. Staecker H, Praetorius M, Baker K, Brough DE. Vestibular hair cell regeneration and restoration of balance function induced by math1 gene transfer. Otol Neurotol. 2007; 28(2):223–31. [PubMed: 17255891]
8. Gubbels SP, Woessner DW, Mitchell JC, Ricci AJ, Brigande JV. Functional auditory hair cells produced in the mammalian cochlea by in utero gene transfer. Nature. 2008; 455(7212):537–41. [PubMed: 18754012]

9. Lalwani AK, Walsh BJ, Reilly PG, Muzyczka N, Mhatre AN. Development of in vivo gene therapy for hearing disorders: introduction of adeno-associated virus into the cochlea of the guinea pig. Gene Ther. 1996; 3(7):588–92. [PubMed: 8818645]
10. Dazert S, Battaglia A, Ryan AF. Transfection of neo-natal rat cochlear cells in vitro with an adenovirus vector. Int J Dev Neurosci. 1997; 15:595–600. [PubMed: 9263036]
11. Lalwani AK, Walsh BJ, Carvalho GJ, Muzyczka N, Mhatre AN. Expression of adeno-associated virus integrated transgene within the mammalian vestibular organs. Am J Otol. 1998; 19:390–395. [PubMed: 9596192]
12. Kiernan AE, Fekete DM. In vivo gene transfer into the embryonic inner ear using retroviral vectors. Audiol Neurootol. 1997; 2(1–2):12–24. [PubMed: 9390818]
13. Weiss MA, Frisancho JC, Roessler BJ, Raphael Y. Viral-mediated gene transfer in the cochlea. Int J Dev Neurosci. 1997; 15(4–5):577–83. [PubMed: 9263034]
14. Lalwani A, Walsh B, Reilly P, Carvalho G, Zolotukhin S, Muzyczka N, et al. Long-term in vivo cochlear transgene expression mediated by recombinant adeno-associated virus. Gene Ther. 1998; 5(2):277–81. [PubMed: 9578849]
15. Derby ML, Sena-Esteves M, Breakefield XO, Corey DP. Gene transfer into the mammalian inner ear using HSV-1 and vaccinia virus vectors. Hear Res. 1999; 134(1–2):1–8. [PubMed: 10452370]
16. Holt JR, John DC, Wang S, Chen ZY, Dunn RI, Marban E, et al. Functional expression of exogenous proteins in mammalian sensory hair cells infected with adenoviral vectors. J Neurophysiol. 1999; 81:1881–1888. [PubMed: 10200223]
17. Van de Water TR, Staecker H, Halterman MW, Federoff HJ. Gene therapy in the inner ear. Mechanisms and clinical implications. Ann N Y Acad Sci. 1999; 884:345–60. [PubMed: 10842605]
18. Yamasoba T, Yagi M, Roessler BJ, Miller JM, Raphael Y. Inner ear transgene expression after adenoviral vector inoculation in the endolymphatic sac. Hum Gene Ther. 1999; 10(5):769–74. [PubMed: 10210144]
19. Chen X, Frisina RD, Bowers WJ, Frisina DR, Federoff HJ. HSV amplicon-mediated neurotrophin-3 expression protects murine spiral ganglion neurons from cisplatin-induced damage. Mol Ther. 2001; 3(6):958–63. [PubMed: 11407910]
20. Jero J, Mhatre AN, Tsend CJ, Stern RE, Coling DE, Goldstein JA, et al. Cochlear gene delivery through an intact round window membrane in mouse. Hum Gene Ther. 2001; 12:539–548. [PubMed: 11268286]
21. Kawamoto K, Oh SH, Kanzaki S, Brown N, Raphael Y. The functional and structural outcome of inner ear gene transfer via the vestibular and cochlear fluids in mice. Mol Ther. 2001; 4(6):575–85. [PubMed: 11735342]
22. Staecker H, Li D, O'Malley BW Jr, Van de Water TR. Gene expression in the mammalian cochlea: a study of multiple vector systems. Acta Otolarngol. 2001; 121:157–163.
23. Luebke AE, Foster PK, Muller CD, Peel AL. Cochlear function and transgene expression in the guinea pig cochlea, using adenovirus- and adeno-associated virus-directed gene transfer. Hum Gene Ther. 2001; 12(7):773–81. [PubMed: 11339894]
24. Ishimoto S, Kawamoto K, Kanzaki S, Raphael Y. Gene transfer into supporting cells of the organ of Corti. Hear Res. 2002; 173(1–2):187–97. [PubMed: 12372646]
25. Liu Y, Okada T, Sheykholeslami K, Shimazaki K, Nomoto T, Muramatsu S, Kanazawa T, Takeuchi K, Ajalli R, Mizukami H, Kume A, Ichimura K, Ozawa K. Specific and efficient transduction of cochlear inner hair cells with recombinant adeno-associated virus type 3 vector. Mol Ther. 2005; 12(4):725–33. [PubMed: 16169458]
26. Stone IM, Lurie DI, Kelley MW, Poulsen DJ. Adeno-associated virus-mediated gene transfer to hair cells and support cells of the murine cochlea. Mol Ther. 2005; 11(6):843–8. [PubMed: 15922954]
27. Bedrosian JC, Gratton MA, Brigande JV, Tang W, Landau J, et al. In vivo delivery of recombinant viruses to the fetal murine cochlea: transduction characteristics and long-term effects on auditory function. Mol Ther. 2006; 14(3):328–35. [PubMed: 16765094]

28. Cooper LB, Chan DK, Roediger FC, Shaffer BR, Fraser JF, Musatov S, et al. AAV-mediated delivery of the caspase inhibitor XIAP protects against cisplatin ototoxicity. Otol Neurotol. 2006; 27(4):484–90. [PubMed: 16791039]
29. Kesser BW, Hashisaki GT, Fletcher K, Eppard H, Holt JR. An in vitro model system to study gene therapy in the human inner ear. Gene Ther. 2007; 14(15):1121–31. [PubMed: 17568767]
30. Venail F, Wang J, Ruel J, Ballana E, Rebillard G, Eybalin M, Arbones M, Bosch A, Puel JL. Coxsackie adenovirus receptor and alpha nu beta3/alpha nu beta5 integrins in adenovirus gene transfer of rat cochlea. Gene Ther. 2007; 14:30–37. [PubMed: 16886000]
31. Wenzel GI, Xia A, Funk E, Evans MB, Palmer DJ, Ng P, Pereira FA, Oghalai JS. Helper-dependent adenovirus-mediated gene transfer into the adult mouse cochlea. Otol Neurotol. 2007; 28(8):1100–8. [PubMed: 18043435]
32. Iizuka T, Kanzaki S, Mochizuki H, Inoshita A, Narui Y, Furukawa M, et al. Noninvasive in vivo delivery of transgene via adeno-associated virus into supporting cells of the neonatal mouse cochlea. Hum Gene Ther. 2008; 19(4):384–90. [PubMed: 18439125]
33. Luebke, A.; Rova, C.; Doersten, P.; Poulsen, D. Adenoviral and AAV-Mediated gene transfer to the inner ear: role of serotype, promoter, and viral load on in vivo and in vitro infection efficiencies. In: Ryan, A., editor. Gene Therapy of Cochlear Deafness. Vol. 66. Basel: Karger; 2009. p. 87-98.
34. Kesser, B.; Anil, Lalwani. Gene therapy and stem cell transplantation: strategies for hearing restoration. In: Ryan, A., editor. Gene Therapy of Cochlear Deafness. Vol. 66. Basel: Karger; 2009. p. 64-86.
35. Husseman, J.; Raphael, Y. Gene therapy in the inner ear using adenovirus vectors. In: Ryan, A., editor. Gene Therapy of Cochlear Deafness. Vol. 66. Basel: Karger; 2009. p. 37-51.
36. Ryan, A.; Mullen, L.; Doherty, J. Cellular targeting for cochlear gene therapy. In: Ryan, A., editor. Gene Therapy of Cochlear Deafness. Vol. 66. Basel: Karger; 2009. p. 99-115.
37. Shibata SB, Di Pasquale G, Cortez SR, Chiorini JA, Raphael Y. Gene transfer using bovine adeno-associated virus in the guinea pig cochlea. Gene Ther. 2009; 16(8):990–7. [PubMed: 19458651]
38. Hankenson FC, Wathen AB, Eaton KA, Miyazawa T, Swiderski DL, Raphael Y. Guinea pig adenovirus infection does not inhibit cochlear transfection with human adenoviral vectors in a model of hearing loss. Comp Med. 2010; 60(2):130–5. [PubMed: 20412688]
39. Praetorius M, Brough DE, Hsu C, Plinkert PK, Pfannenstiel SC, Staecker H. Adenoviral vectors for improved gene delivery to the inner ear. Hear Res. 2009; 248(1–2):31–8. [PubMed: 19105978]
40. Praetorius M, Hsu C, Baker K, Brough DE, Plinkert P, Staecker H. Adenovector-mediated hair cell regeneration is affected by promoter type. Acta Otolaryngol. 2010; 130(2):215–22. [PubMed: 20095092]
41. Taura A, Taura K, Choung YH, Masuda M, Pak K, Chavez E, Ryan AF. Histone deacetylase inhibition enhances adenoviral vector transduction in inner ear tissue. Neuroscience. 2010; 66(4): 1185–93. [PubMed: 20060033]
42. Luebke AE, Steiger JD, Hodges BL, Amalfitano A. A modified adenovirus can transfect cochlear hair cells in vivo without compromising cochlear function. Gene Ther. 2001; 8(10):789–94. [PubMed: 11420643]
43. Liu Y, Okada T, Nomoto T, Ke X, Kume A, Ozawa K, Xiao S. Promoter effects of adeno-associated viral vector for transgene expression in the cochlea in vivo. Exp Mol Med. 2007; 39(2): 170–5. [PubMed: 17464178]
44. Auricchio A, O'Connor E, Hildinger M, Wilson JM. A single-step affinity column for purification of serotype-5 based adeno-associated viral vectors. Mol Ther. 2001; 4:372–374. [PubMed: 11592841]
45. Oesterle EC, Campbell S, Taylor RR, Forge A, Hume CR. Sox2 and JAGGED1 expression in normal and drug-damaged adult mouse inner ear. J Assoc Res Otolaryngol. 2008; 9(1):65–89. [PubMed: 18157569]
46. Ding, D.; McFadden, SL.; Salvi, RJ. Cochlear hair cell densities and inner-ear staining techniques. In: Willott, JF., editor. Handbook of mouse auditory research. New York: CRC; 2001.

47. Lang H, Schulte BA, Zhou D, Smythe N, Spicer SS, Schmiedt RA. Nuclear factor kappaB deficiency is associated with auditory nerve degeneration and increased noise-induced hearing loss. J Neurosci. 2006; 26(13):3541–50. [PubMed: 16571762]
48. Chalfie M, Tu Y, Euskirchen G, Ward WW, Prasher DC. Green fluorescent protein as a marker for gene expression. Science. 1994; 263(5148):802–5. [PubMed: 8303295]
49. Taylor RR, Nevill G, Forge A. Rapid hair cell loss: a mouse model for cochlear lesions. J Assoc Res Otolaryngol. 2008; 9(1):44–64. [PubMed: 18057986]
50. Oesterle EC, Campbell S. Supporting cell characteristics in long-deafened aged mouse ears. J Assoc Res Otolaryngol. 2009; 10(4):525–44. [PubMed: 19644644]
51. Thorne M, Salt AN, DeMott JE, Henson MM, Henson OW Jr, Gewalt SL. Cochlear fluid space dimensions for six species derived from reconstructions of three-dimensional magnetic resonance images. Laryngoscope. 1999; 109(10):1661–8. [PubMed: 10522939]
52. Chen Z, Mikulec AA, McKenna MJ, Sewell WF, Kujawa SG. A method for intracochlear drug delivery in the mouse. Neurosci Methods. 2006; 150(1):67–73.
53. Borkholder DA, Zhu X, Hyatt BT, Archilla AS, Livingston WJ, Frisina RD. murine intracochlear drug delivery: reducing concentration gradients within the cochlea. Hear Res. 2010 In Press.
54. Lang H, Schulte BA, Schmiedt RA. Endocochlear potentials and compound action potential recovery functions in the C57BL/6J mouse. Hear Res. 2002; 172(1–2):118–26. [PubMed: 12361874]
55. Hester ME, Foust KD, Kaspar RW, Kaspar BK. AAV as a gene transfer vector for the treatment of neurological disorders: novel treatment thoughts for ALS. Curr Gene Ther. 2009; 9(5):428–33. [PubMed: 19860657]
56. Summerford C, Samulski RJ. Membrane-associated heparan sulfate proteoglycan is a receptor for adeno-associated virus type 2 virions. J Virol. 1998; 72(2):1438–45. [PubMed: 9445046]
57. Summerford C, Bartlett JS, Samulski RJ. AlphaVbeta5 integrin: a co-receptor for adeno-associated virus type 2 infection. Nat Med. 1999; 5(1):78–82. [PubMed: 9883843]
58. Akache B, Grimm D, Pandey K, Yant SR, Xu H, Kay MA. The 37/67-kilodalton laminin receptor is a receptor for adeno-associated virus serotypes 8, 2, 3, and 9. J Virol. 2006; 80(19):9831–6. [PubMed: 16973587]
59. Negishi A, Chen J, McCarty DM, Samulski RJ, Liu J, Superfine R. Analysis of the interaction between adeno-associated virus and heparan sulfate using atomic force microscopy. Glycobiology. 2004; 14(11):969–77. [PubMed: 15215232]
60. Spicer SS, Schulte BA. The fine structure of spiral ligament cells relates to ion return to the stria and varies with place-frequency. Hear Res. 1996; 100(1–2):80–100. [PubMed: 8922982]
61. Steel KP. Perspectives: biomedicine. The benefits of recycling. Science. 1999; 285(5432):1363–4. [PubMed: 10490411]
62. Minowa O, Ikeda K, Sugitani Y, Oshima T, Nakai S, Katori Y, Suzuki M, Furukawa M, Kawase T, Zheng Y, Ogura M, Asada Y, Watanabe K, Yamanaka H, Gotoh S, Nishi-Takeshima M, Sugimoto T, Kikuchi T, Takasaka T, Noda T. Altered cochlear fibrocytes in a mouse model of DFN3 nonsyndromic deafness. Science. 1999; 285(5432):1408–11. [PubMed: 10464101]
63. Shibata SB, Cortez SR, Beyer LA, Wiler JA, Di Polo A, Pfingst BE, Raphael Y. Transgenic BDNF induces nerve fiber regrowth into the auditory epithelium in deaf cochleae. Exp Neurol. 2010; 223(2):464–72. [PubMed: 20109446]

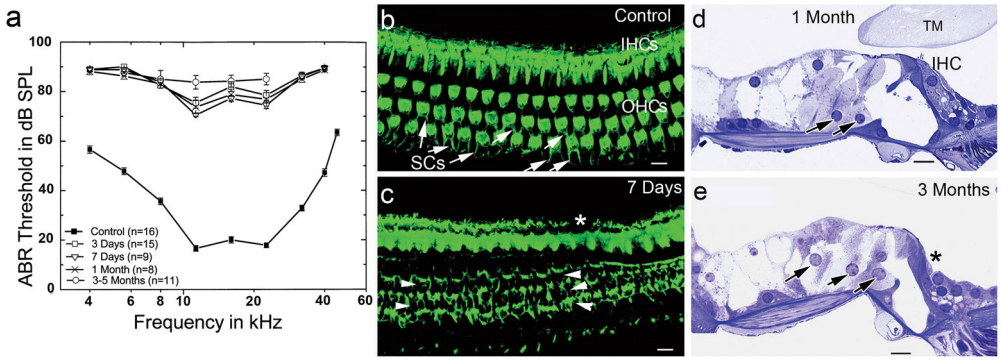

Figure 1.

Hair cell degeneration and severe hearing loss induced by kanamycin and furosemide (K+F) treatment in adult CBA/CaJ mice. **(a)** Mean ABR thresholds in mice tested at 3 days, 7 days, 1 month and 3–5 months post-deafening. Data are expressed as mean ± SEM. ABR thresholds in all treated groups were elevated by 40 to 70 dB SPL across the frequencies. Note there were no responses at 90 dB SPL with 32 and 40 kHz probe tones in mice tested at 3–5 months after treatment. **(b)** Surface preparation shows stereocilia of IHCs and OHCs and part of the apical regions of supporting cells (SCs, arrows) stained with FITC-phalloidin. The image was taken from the middle turn of a normal CBA/CaJ adult mouse. **(c)** All OHCs are lost in the middle turn of a K+F treated mouse allowed to recover for 7 days. SC scars appear in all three rows of OHC region (arrowheads). One IHC is lost (*). **(d)** OHCs are missing in a plastic-embedded cross section of the upper basal turn. Swollen and disorganized Deiter's cells are present (black arrows). **(e)** IHCs and OHCs are lost in a section taken from the upper basal turn. Enlarged Deiter's cells appear in the OHC region. An IHC is missing (*). TM, tectorial membrane. Scale bars =10 μm in (b,c,d,e).

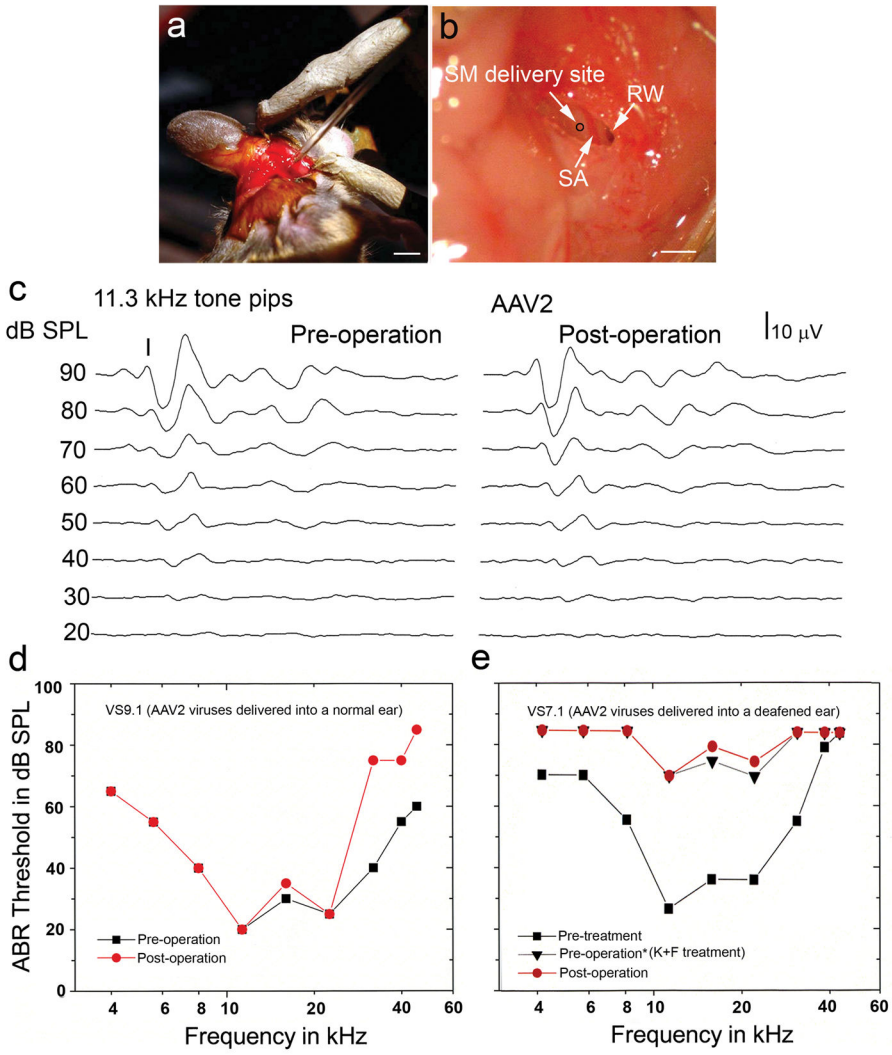

Figure 2.

AAV inoculation into the scala media (SM) of normal and deafened adult mice with minor surgical trauma. **(a)** A post-auricular surgical approach for delivering AAV vectors into the adult mouse cochlea using a glass micropipette. **(b)** Surgical approach to expose the SM delivery site (black circle), stapedial artery (SA) and round window (RW). Note that the bony lateral wall of the virus delivery site was thinned by dental drilling before a virus-loaded glass pipette is maneuvered into the SM. **(c)** ABR intensity series for tone pips at 11.3 kHz were recorded pretreatment and 1 month after type AAV2 virus was delivered into a normal adult mouse cochlea (VS9.1). **(d)** Slightly increased ABR threshold shifts were seen at high frequencies in the mouse shown in (c). **(e)** ABR thresholds in an adult mouse (VS7.1) before K+F treatment, after K+F treatment (listed as pre-operation in the figure) and 7 days after AAV2 inoculation. Increased thresholds across all frequencies appeared after K+F treatment, but minimal change in ABR threshold occurred after virus inoculation. Note that IHC transduction of the organ of Corti obtained from this mouse is shown in Figure 4c. Scale bars: (a), 3 mm; (b), 1mm.

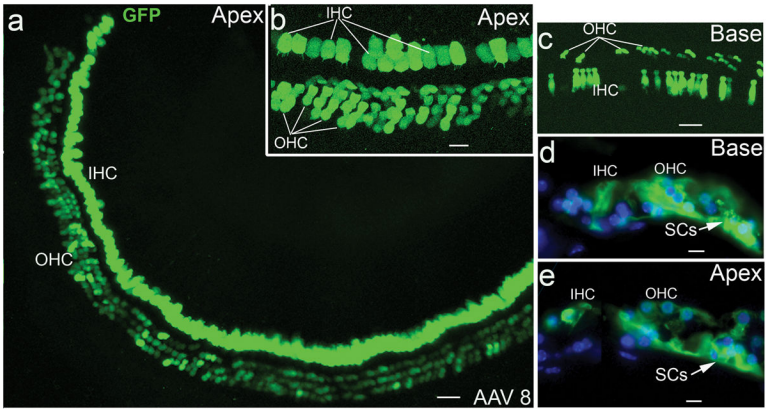

Figure 3.

AAV-GFP transduction in hair cells of normal adult mice. **(a)** AAV-GFP transduction in IHC and OHC areas of the apical turn of a mouse 7 days after virus inoculation. **(b)** Higher magnification view of the GFP^+ cells in the apical turn shown in (a). **(c)** GFP^+ IHCs and OHCs in the basal turn of the mouse shown in (a). GFP^+ IHCs, OHCs and SCs in cross-sections of the apical **(d)** and basal turns **(e)** in a normal mouse one month after virus inoculation. Note that all images show the AAV transduction for serotype 8. Scale bars: (a) and (c), 30 μm; (b), 20 μm; (d) and (e), 10 μm.

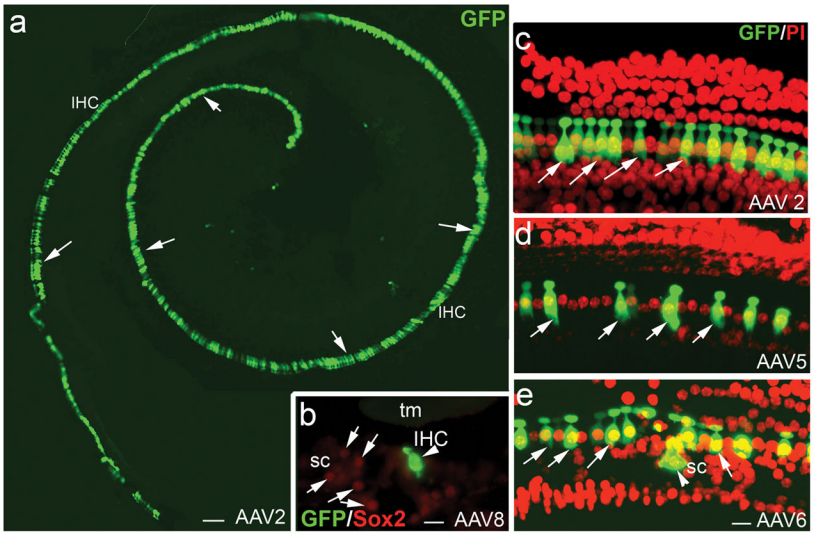

Figure 4.

AAV-GFP transduction in IHCs of deafened mouse ears. **(a)** AAV-GFP transduction of IHCs (arrows) in the cochlea of a deafened mouse 7 days after virus inoculation with serotype 2 vector. **(b)** AAV-GFP transduction in an IHC (arrowhead) of the apical turn in a cross-section of the organ of Corti with serotype 8. The specimen was taken from a deafened mouse one month after virus inoculation. SCs (arrows) were identified by positive staining for Sox2 (red, supporting cell marker). **(c–e)** AAV-GFP transduction patterns in the organ of Corti of deafened ears with the nuclear counterstain propidium iodide (PI, red). The specimens taken were from mice 7 days after virus inoculation. GFP^+ IHCs (arrows) were seen in the basal turns of deafened mice for serotype 2 (c), serotype 5 (d) and serotype 6 (e). A SC (arrowhead) was effectively transduced by serotype 6 as seen in (e). Note that the deafened mice were induced with K+F and allow to recover for 3 days (a, c), 6 months (b) and 1 month (d, e). tm, tectorial membrane; sc, supporting cells. Scale bars: (a), 50 μm; (b), 20 μm; (c–e), 20 μm.

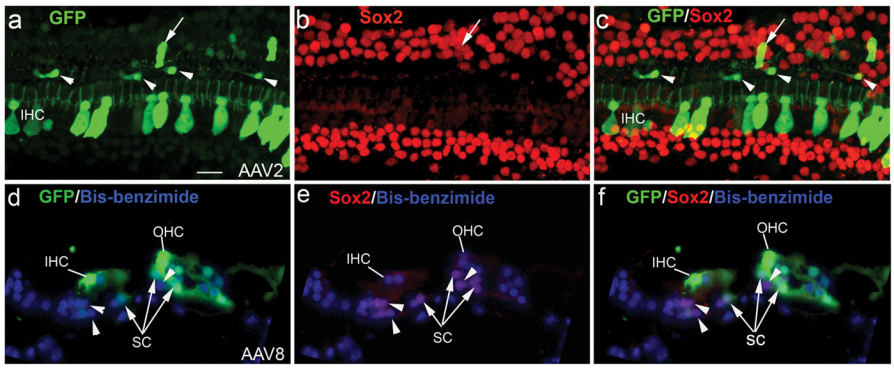

Figure 5.

A small number of SCs transduced with AAV-GFP vectors. **(a–c)** Double labeling for GFP (green) and Sox2 (red) in a deafened mouse inoculated with serotype 2. This mouse was allowed to recover for 7 days after drug delivery and before virus inoculation. One GFP^+/$Sox2^+$ SC is indicated by a white arrow. The white arrowheads show four $Sox2^-$/GFP^+ cells with fibroblast-like morphology. (d–f) Double labeling for GFP (green) and Sox2 (red) in a control mouse one month after serotype 8 inoculation. A few GFP^+/$Sox2^+$ SCs (arrows) are present in a cross section of the basal turn. A GFP^+ IHC, a GFP^+ OHC and three GFP^-/$Sox2^+$SCs (arrowheads) are also shown. Note that nuclei were counterstained with bisbenzimide (blue). Scale bar = 25 μm (a–f).

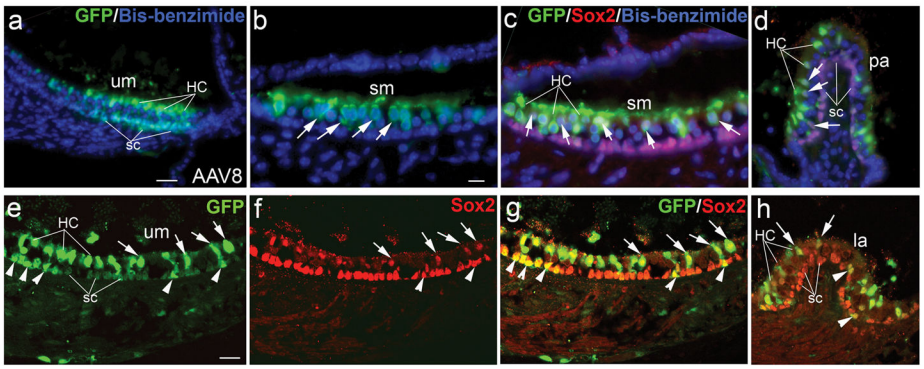

Figure 6.

AAV-GFP transduction in the sensory epithelia of the vestibular organs in normal and deafened mice for serotype 8. **(a)** GFP^+ cells in the HC and SC layers of the utricular macula in a normal mouse one month after virus inoculation. **(b)** GFP expression in HCs (arrows) of the saccular macula in the mouse shown in (a). **(c)** GFP^+ cells in the HC layer of the saccular macula in a deafened mouse one month after virus inoculation. The majority of GFP^+ cells in the HC layer were colabeled with Sox2 (arrows). **(d)** $Sox2^+/GFP^+$ cells in the sensory epithelium of the posterior ampulla of the mouse shown in (c). Note that nuclei were counterstained with bisbenzimide in a–d. **(e-g)** Confocal images revealed $Sox2^+/GFP^+$ HCs (arrows) and SCs (arrowheads) in the sensory epithelium of the utricular macular of the mouse shown in (c). **(h)** Confocal images revealed $Sox2^+/GFP^+$ HCs (arrows) and SCs (arrowheads) in the sensory epithelium of the lateral ampulla of the mouse shown in (c). Note that this deafened mouse was treated with K+F and allowed to recover for 1 month (c–h). la, lateral ampulla; pa, posterior ampula; sm, saccular macula; um, utricular macula. Scale bars: (a), 50 μm; (b–d), 20 μm; (e–h), 30 μm.

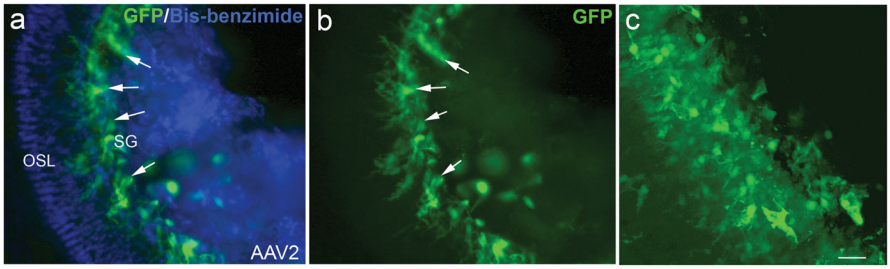

Figure 7.

AAV-GFP transduction in the auditory nerve of a normal mouse.

(a, b) GFP^+ cells (arrows) within Rosenthal's canal of a normal mouse 7 days after virus inoculation with serotype 2. Nuclei were counterstained with bis-benzimide (blue). **(c)** Confocal image of GFP^+ cells within Rosenthal's canal of the mouse shown in (a). The image was rebuilt with 33 continuous individual images using the Projection feature of Zeiss LSM Image Browser software 4.2. OSL, osseous spiral lamina; SG, spiral ganglion. Scale bar = 30 μm (b,c).

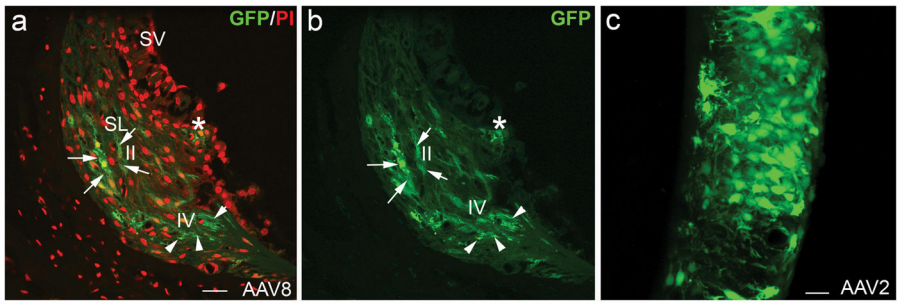

Figure 8.

AAV-GFP transduction in the cochlear lateral wall of normal and deafened mice. **(a, b)** GFP^+ cells in the spiral ligament of the basal turn of a normal mouse one month after virus inoculation with serotype 8. These GFP^+ cells are located among the outer sulcus epithelial cells (*) and types II (II, arrows) and IV (IV, arrowheads) fibrocytes of the spiral ligament. Nuclei were counterstained with PI. **(c)** Confocal image of GFP^+ cells in the upper basal turn of a deafened mouse 7 days after virus inoculation with serotype 2. The confocal image is a z-projection of 16 continuous individual images taken from a whole mount preparation. The mouse was deafened with K+F and allowed to recover for 3 days before the virus inoculation. SL, spiral ligament; SV, stria vascularis. Scale bars: (a, b), 20 μm; (c), 15 μm.

Table 1

Transduction efficiency of AAV-GFP vectors in the mouse cochleae.

Serotype	1	2	5	6	8	Total
Control	3/4 (1/4)	**14/14 (7/14)**	3/4 (0/4)	4/5 (4/5)	**11/12 (4/12)**	35/39 (16/39) 89.7% (41%)
Acute K + F 3−7d	3/4 (0/4)	**11/12 (6/12)**	2/5 (0/5)	3/3 (0/3)	**13/13 (8/13)**	32/37 (14/37) 86.5% (37.8%)
Chronic K + F 1−6 m	1/3 (1/3)	**4/6 (1/6)**	1/3 (0/3)	2/3 (0/3)	**9/10 (2/10)**	17/25 (5/25) 68% (21.7%)
Total	7/11 (2/11) 63.6% (18.2%)	**29/32 (14/32)** **90.6% (43.8%)**	6/12 (0/12) 50% (0%)	9/11 (4/11) 82% (36.4%)	**33/35 (14/35)** **94.3% (40%)**	84/101 (34/101) 83.1% (33.7%)

The values shown are the number of mice with IHC GFP expression in the inner ears (criterion of at least 3 GFP^+IHCcells shown each ear) compared to the total number of mice inoculated. Proportions in parentheses demonstrate the number of mice with >100 GFP^+ IHCs of the total number of mice inoculated. Serotypes 2 and 8 are most effective at transducing IHCs (note that serotype 6 appears overall effective but no deafened mice expressed >100 GFP^+ IHCs).

Table 2

Transduction efficiency of serotypes 2 and 8 vectors with variable inoculation time.

Serotype	**2**		**8**	
Time after SM inoculation	**7 days**	**1 month**	**7 days**	**1 month**
Control	8/8 (3/8)	6/6 (5/6)	6/6 (1/6)	5/6 (2/6)
Acute (K + F 3−7d)	8/9 (4/9)	3/3 (2/3)	9/9 (5/9)	4/4 (3/4)
Chronic (K + F 1−6m)	3/4 (2/4)	1/2 (0/2)	3/3 (1/3)	6/7 (2/7)
Total	19/21 (9/21) 90.5% (42.9%)	10/11 (7/11) 90.9% (63.6%)	18/18 (7/18) 100% (38.9%)	15/17 (7/17) 88.2% (41.2%)

The values shown are the number of mice with any IHC GFP expression in the inner ears (criterion of at least 3 IHC GFP^+cells in the injected ear) compared to the total number of inoculated mice as well as the number of mice with >100 GFP^+ IHCs compared to the total number of inoculated mice (in parentheses). The bottom row converts these ratios to percentages.

Table 3

Transduction efficiency of AAV-GFP vectors in the auditory nerves of the mouse cochleae.

Serotype	1	2	5	6	8	Total
Control	1/4	4/12	0/4	1/3	**6/10**	12/33 36.3%
Deafened **K + F 3−7d or 1−6 m**	2/3	9/19	2/5	2/5	**12/20**	27/52 51.9%
Total	3/7 42.9%	13/31 41.9%	2/9 22.2%	3/8 37.5%	**18/30** **60%**	39/85 (34/101) 83.1% (33.7%)

The values shown are the number of mice with GFP expression in the spiral ganglion on the injected side compared to the total number of mice observed. The bottom row converts these ratios to percentages.